DHI ref. 58/91

Coastal Engineering, 15 (1991) 371–388
Elsevier Science Publishers B.V., Amsterdam

A new form of the Boussinesq equations with improved linear dispersion characteristics

Per A. Madsen[1], Russel Murray[2] and Ole R. Sørensen[1]
[1]*Danish Hydraulic Institute, Agern Allé 5, DK-2970 Hørsholm, Denmark*
[2]*Department of Harbours and Marine, Brisbane, Australia*

(Received May 1, 1990; accepted after revision December 4, 1990)

ABSTRACT

Madsen, P.A., Murray, R. and Sørensen, O.R., 1991. A new form of the Boussinesq equations with improved linear dispersion characteristics. *Coastal Eng.*, 15: 371–388.

A new form of the Boussinesq equations is introduced in order to improve their dispersion characteristics. It is demonstrated that the depth-limitation of the new equations is much less restrictive than for the classical forms of the Boussinesq equations, and it is now possible to simulate the propagation of irregular wave trains travelling from deep water to shallow water. In deep water, the new equations become effectively linear and phase celerities agree with Stokes first-order theory. In more shallow water, the new equations converge towards the standard Boussinesq equations, which are known to provide good results for waves up to at least 75% of their breaking height. A numerical method for solving the new set of equations in two horizontal dimensions is presented. This method is based on a time-centered implicit finite-difference scheme. Finally, model results for wave propagation and diffraction in relatively deep water are presented.

1 INTRODUCTION

Numerical models based on the two-dimensional Boussinesq equations have been shown to be capable of reproducing the combined effects of most of the wave phenomena of interest to the coastal engineer (Madsen and Warren, 1983; Larsen et al., 1984; Berenguer et al., 1986; Yu Kuang-ming et al., 1987). These include shoaling, refraction, diffraction and partial reflection of directional, irregular, finite-amplitude waves propagating over complex bathymetries.

The Boussinesq equations include non-linearity as well as frequency dispersion. Basically, the frequency dispersion is introduced in the flow equations by taking into account the effect that vertical accelerations (or the curvature of the streamlines) have on the pressure distribution. The simplest way of including this effect in the vertically integrated momentum equations is to assume a horizontal velocity distribution which is uniform throughout

the depth. This leads to a vertical velocity distribution which increases linearly from zero at the bed to a maximum at the free surface. However, there are other methods available to derive the Boussinesq equations, and a variety of different forms exist (Peregrine, 1967, 1974; Svendsen, 1974; McCowan, 1985).

First of all, the dependent variables can be chosen in different ways, and typical velocity variables are the surface velocity, the bottom velocity, the depth-averaged velocity and the depth-integrated velocity. Secondly, since the nonlinear and dispersive terms are of higher order, they can be manipulated by invoking the long-wave equation. Examples of this manipulation have been given by e.g. Mei (1983), presenting four different forms of the KdV equation. Common for all the standard forms of the Boussinesq equations is that all products of derivatives have been neglected relative to the derivatives themselves. Serre (1953), on the other hand, retained the additional terms arising from the convective terms in the expression for the vertical velocity, the convective terms in the vertical flow equation and bed slope effects. However, this does not make the Serre equations more accurate or complete than the more simple forms of the Boussinesq equations because Serre's derivation strictly relies on the assumption of a uniform vertical distribution of the horizontal velocity.

The practical range of application of the various forms of the Boussinesq equations has been studied in detail by McCowan (1981, 1985, 1987). He has demonstrated that the form of the coefficient for the third derivative Boussinesq term, P_{xxt}, is highly relevant for modelling nonlinear waves in shallow water. The optimal choice has been shown to be h^2, where h is the still water depth (McCowan, 1985). By using this coefficient and including only the P_{xxt} Boussinesq term, McCowan (1987) achieved excellent agreement with the stream function solutions of Chaplin (1980) for waves almost up to their breaking height.

The major restriction of the Boussinesq equations is their water-depth limitation: The worst forms of the equations break down for depth to deep-water wave-length ratios (h/L_0) larger than 0.12 while the best forms are limited to about 0.22, corresponding to a 5% celerity error.

For many applications, a less restrictive water-depth limitation is desirable. This requirement of an improved linear dispersion property in deeper water has been addressed by Witting (1984), who presented a new set of equations valid for a single horizontal dimension. Unfortunately, it is far from straightforward to generalize Witting's approach to two horizontal dimensions.

This paper presents a new form of the Boussinesq equations valid for irregular wave trains in two horizontal dimensions. From a computational point of view, the new equations are only slightly different from the standard equations solved by Abbott et al. (1978). However, the new equations incorporate a significant improvement of the phase celerity and group velocity properties

for the linear waves in water depths up to the deep water limit and beyond. The presentation starts with a review of the linear dispersion properties of the various classical forms of the Boussinesq equations in Section 2. The new set of equations are formulated in Section 3, the numerical solution method is explained in Section 4, and finally the model results are discussed in Section 5.

2 LINEAR DISPERSION PROPERTIES OF VARIOUS FORMS OF THE BOUSSINESQ EQUATIONS

In the following, the depth limitations of the different existing forms of the Boussinesq equations will be determined. For this purpose, only the linearized reduction of the various equations will be considered and the corresponding phase celerities and group velocities will be compared to Stokes first-order theory. Only one horizontal coordinate will be considered for this purpose and, furthermore, the bottom will be assumed to be horizontal.

Various forms of the equations

In the introduction, one way of deriving the Boussinesq equations was described. Here, a different method will be chosen because it provides a simple way of illustrating the most common forms of the Boussinesq equations including the approach by Witting. First of all, the depth-integrated continuity equation and the Bernoulli equation for the surface velocity (U_s) will be taken as a starting point of the derivation of the equations:

$$\left.\begin{aligned} &S_t+(\bar{U}h)_x=0 \\ &U_{s_t}+gS_x=0 \end{aligned}\right| \qquad (1)$$

where S is the surface elevation, $\bar{U}$ the depth-averaged velocity, U_s the surface velocity, h the still water depth, and the suffices t and x denote partial differentiation with respect to time and space. In order to close the equations, a relation between the depth-averaged velocity and the surface velocity is necessary. This, however, requires detailed knowledge of the vertical distribution of the horizontal velocity. The classical way of obtaining this distribution is to apply a Taylor expansion about the bottom and to express the velocity in terms of the bottom velocity, U_b (see Svendsen, 1974, or Witting, 1984):

$$U=U_b-\frac{1}{2}(z+h)^2U_{b_{xx}}+\frac{1}{24}(z+h)^4U_{b_{xxxx}}+\ldots \qquad (2a)$$

where z is the vertical coordinate.

By using Eq. 2a, the following expressions can be derived for the depth-averaged velocity, $\bar{U}$, and for the surface velocity U_s:

$$\bar{U}=U_b-\frac{1}{6}h^2U_{bxx}+\frac{1}{120}h^4U_{bxxxx}+... \tag{2b}$$

$$U_s=U_b-\frac{1}{2}h^2U_{bxx}+\frac{1}{24}h^4U_{bxxxx}+... \tag{2c}$$

Notice that no additional assumptions have been introduced in the derivation of Eqs. 2a–c; hence in that respect the equations are exact (Witting, 1984). On the other hand, the infinite-series solutions are of little use if they are not truncated, and this can only be done if the higher-order derivative terms effectively are of higher order, i.e., if the wave number, k, is small or moderate. This is exactly where the shallow water assumption comes in. For the present purpose, the series will be truncated after the second derivative terms, i.e.:

$$\bar{U}\approx U_b-\frac{1}{6}h^2U_{bxx} \tag{3a}$$

$$U_s\approx U_b-\frac{1}{2}h^2U_{bxx} \tag{3b}$$

Substituting Eq. 3a and Eq. 3b into Eq. 1 leads to:

$$\begin{aligned} &S_t+hU_{bx}-\frac{1}{6}h^3U_{bxxx}=0\\ &U_{bt}+gS_x-\frac{1}{2}h^2U_{bxxt}=0 \end{aligned} \tag{4}$$

which is just one possible form of the Boussinesq equations (Svendsen, 1974).

An alternative form of the Boussinesq equations can be derived in terms of the surface velocity, U_s. Firstly Eq. 3b is solved with respect to U_b:

$$U_b\approx U_s+\frac{1}{2}h^2U_{sxx} \tag{5}$$

Secondly this result is substituted into Eq. 4 and the resulting equations (also reported by Svendsen, 1974) become:

$$\begin{aligned} &S_t+hU_{sx}+\frac{1}{3}h^3U_{sxxx}=0\\ &U_{st}+gS_x=0 \end{aligned} \tag{6}$$

A third form of the Boussinesq equations can be derived in terms of the mean velocity, $\bar{U}$. Now Eq. 3a is solved with respect to U_b:

$$U_b \approx \bar{U} + \frac{1}{6} h^2 \bar{U}_{xx} \tag{7}$$

and combining this with Eq. 5 leads to:

$$U_s \approx \bar{U} - \frac{1}{3} h^2 \bar{U}_{xx} \tag{8}$$

Substituting Eq. 8 into Eq. 1 finally yields:

$$\begin{aligned} &S_t + h\bar{U}_x = 0 \\ &\bar{U}_t + gS_x - \frac{1}{3} h^2 \bar{U}_{xxt} = 0 \end{aligned} \tag{9}$$

In principle, this is the form used by Abbott et al. (1984) and suggested by Whitham (1974).

Finally, Witting (1984) introduced a new type of Boussinesq equations which, among other enhancements, incorporated improved dispersion characteristics. In the following, a linearized form of his equations will be considered. First of all, Witting replaced the straightforward Taylor expansion in Eqs. 2b–c by the following expansions:

$$\begin{aligned} \bar{U} &= \hat{U} - b^{(1)} h^2 \hat{U}_{xx} + b^{(2)} h^4 \hat{U}_{xxxx} + \ldots \\ U_s &= \hat{U} - a^{(1)} h^2 \hat{U}_{xx} + a^{(2)} h^4 \hat{U}_{xxxx} + \ldots \end{aligned} \tag{10}$$

Notice that the bottom velocity has been replaced by the pseudo velocity $\hat{U}$ and the Taylor coefficients have been replaced by calibration coefficients used to optimize the accuracy of the phase celerity. For the present purpose, the infinite series are once again truncated after the second derivative terms, and substituting Eq. 10 into Eq. 1 leads to:

$$\begin{aligned} &S_t + h\hat{U}_x - b^{(1)} h^3 \hat{U}_{xxx} = 0 \\ &\hat{U}_t + gS_x - a^{(1)} h^2 \hat{U}_{xxt} = 0 \end{aligned} \tag{11}$$

Witting (1984) did not actually solve the equations on this form, but Eq. 11 merely serves as a practical way of illustrating Witting's approach.

Phase celerity

In order to derive the dispersion relations corresponding to the various forms of the Boussinesq equations, the following standard procedure is followed. First of all, the wave is assumed to be of constant form, i.e., a phase function $\theta(x,t)$ exists and the local wave number, k, the angular wave frequency, ω, and the celerity, c, is determined by:

$$k=\theta_x, \quad \omega=-\theta_t, \quad c=\frac{\omega}{k} \tag{12}$$

By eliminating S from Eqs. 4, 6, 9 and 11, and using Eq. 12, the phase celerities can be determinated corresponding to each of the forms of the Boussinesq equations:

$$\frac{c^2}{gh}=\frac{1+\frac{1}{6}k^2h^2}{1+\frac{1}{2}k^2h^2} \qquad \text{(from Eq. 4)} \tag{13a}$$

$$\frac{c^2}{gh}=1-\frac{1}{3}k^2h^2 \qquad \text{(from Eq. 6)} \tag{13b}$$

$$\frac{c^2}{gh}=\frac{1}{1+\frac{1}{3}k^2h^2} \qquad \text{(from Eq. 9)} \tag{13c}$$

$$\frac{c^2}{gh}=\frac{1+b^{(1)}k^2h^2}{1+a^{(1)}k^2h^2} \qquad \text{(from Eq. 11)} \tag{13d}$$

Witting determined the calibration coefficients $a^{(1)}$ and $b^{(1)}$ by matching Eq. 13d with a Taylor expansion of the Stokes first-order celerity:

$$\frac{c^2}{gh}=\frac{\tanh kh}{kh}\rightarrow 1-\frac{k^2h^2}{3}+\frac{2}{15}k^4h^4+\ldots \tag{14}$$

A Pade's expansion technique gave the coefficients $a^{(1)}=2/5$ and $b^{(1)}=1/15$.

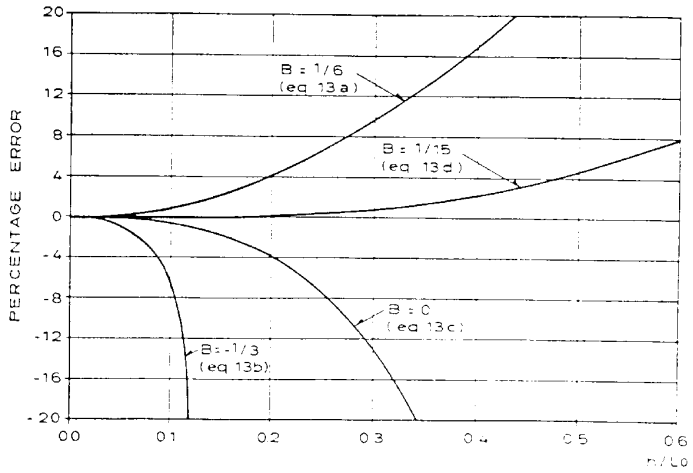

Fig. 1. Percentage errors of the phase celerity for various forms of the Boussinesq equations relative to Stokes first-order theory, i.e., 100 $(c-c_{\text{STOKES}})/c_{\text{STOKES}}$, where c is determined from Eq. 15 and c_{STOKES} from Eq. 14.

It is now observed that each form of the equations leads to a different celerity expression, but for small wave numbers all the derived expressions converge towards the Stokes first-order theory for waves on arbitrary depth, which for this purpose will be considered as the exact solution. As the wave number increases, the various celerity expressions become more and more inaccurate relative to the Stokes theory.

It turns out to be convenient to write the different celerities in the following form:

$$\frac{c^2}{gh} = \frac{1 + Bk^2h^2}{1 + (B + \frac{1}{3})k^2h^2} \tag{15}$$

where:

$$B = \begin{cases} 1/6 & \text{(Eq. 13a using } L_0\text{)} \\ -1/3 & \text{(Eq. 13b using } L_1\text{)} \\ 0 & \text{(Eq. 13c using } L\text{)} \\ 1/15 & \text{(Eq. 13d using Pade's expansion)} \end{cases}$$

So far, the phase celerities have been expressed in terms of the local wave numbers. These wave numbers are determined from the dispersion relation embedded in Eq. 15, and by using the definition:

$$\frac{c^2}{gh} \equiv \frac{\omega^2}{ghk^2} = \frac{h}{L_0}\frac{2\pi}{k^2h^2}$$

we can determine the local wave number and phase celerity as a function of the ratio of the water depth to the deep water wave length, h/L_0.

A comparison with Stokes first-order theory is shown in Fig. 1, presenting the difference between c and c_{STOKES} in percentage of c_{STOKES} for different values of B. It is seen that $B = -1/3$, i.e., Eq. 13b appears to have the poorest phase properties, and for $h/L_0 > 0.12$ solutions to the dispersion relation cannot be found. As remarked by McCowan (1987), this corresponds to the depth limitation for cnoidal wave theory. It is also seen that $B = 0$, i.e., Eq. 13c has the best phase properties of the standard Boussinesq equations. This is the form recommended by Whitham (1974) and applied by most of the existing numerical models today. The absolute water-depth limit beyond which solutions to the dispersion relation cannot be found is $h/L_0 = 0.48$. However, in order to restrict phase errors to, say, 5%, the practical upper limit for h/L_0 reduces to 0.22, which corresponds to the water-depth limit determined numerically by McCowan (1981).

Finally, the form suggested by Witting ($B = 1/15$) is seen to be superior to the other forms. With phase errors restricted to 5%, the practical depth limitation of this method becomes as large as 0.50!

Group velocity

In order to get the full picture of the range of validity of the various equations, it is necessary also to inspect the performance with respect to the group velocity. This will influence the propagation of irregular wave trains and, for the nonlinear case, it will influence the group induced sub- and super-harmonics. Furthermore, the rate at which a model 'warms up' from a cold start depends on the rate at which energy propagates through the model.

The group velocity can be derived by applying the definition:

$$c_g = c + k\frac{\mathrm{d}c}{\mathrm{d}k} \tag{16}$$

where the water depth is kept constant during differentiation. Hence, substituting Eq. 15 into Eq. 16 yields:

$$c_g = c\left[1 + \frac{Bk^2h^2}{1+Bk^2h^2} - \frac{(B+\frac{1}{3})k^2h^2}{1+(B+\frac{1}{3})k^2h^2}\right] \tag{17}$$

The group velocities are determined in two steps. Firstly, the local wave number is determined as a function of h/L_0 by solving the dispersion relation embedded in Eq. 15. Secondly, the result is substituted in Eq. 17.

A comparison with Stokes first-order theory is shown in Fig. 2, presenting the difference between c_g and $c_{g,STOKES}$ in percentage of $c_{g,STOKES}$ for different values of B. The errors are surprisingly large even for relatively shallow water. By restricting the percentage errors to, say, 6% the practical water-depth limitations become:

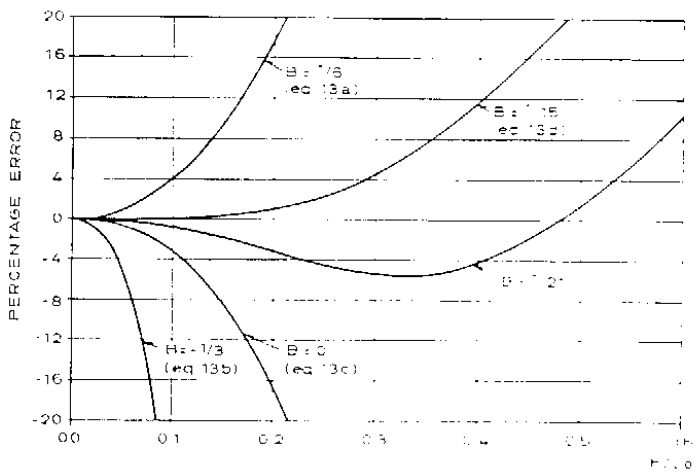

Fig. 2. Percentage errors of the group velocity for various forms of the Boussinesq equations relative to Stokes first-order theory, i.e., $100(c_g - c_{g,STOKES})/c_{g,STOKES}$, where c_g is determined from Eq. 17.

$$h/L_0 = \begin{cases} 0.055 \text{ (for } B = -1/3) \\ 0.12 \text{ (for } B = 1/6) \\ 0.13 \text{ (for } B = 0) \\ 0.32 \text{ (for } B = 1/15) \end{cases}$$

Again Witting's method is superior to the standard forms of the Boussinesq equations. Unfortunately, it turns out to be very difficult to generalize Witting's approach to two horizontal dimensions. Instead, the excellent linear dispersion characteristics achieved by Witting's technique have given the inspiration to develop a new set of Boussinesq equations, which will be presented in the next Section.

3 A NEW SET OF BOUSSINESQ EQUATIONS

It is the intention to formulate a new set of Boussinesq equations which meet the following requirements:

(a) The equations should be expressed in two horizontal dimensions in terms of the surface elevation and the depth-integrated velocity components.

(b) The resulting linear dispersion characteristics should follow Eq. 15, where the coefficient B can be chosen explicitly to improve the accuracy in deeper water.

As a starting point we shall consider the classical form of the Boussinesq equations solved by Abbott et al. (1984):

$$S_t + P_x + Q_y = 0 \tag{18a}$$

$$P_t + \left(\frac{P^2}{d}\right)_x + \left(\frac{PQ}{d}\right)_y + gdS_x - \frac{1}{3}h^2\left(P_{xxt} + Q_{xyt}\right) = 0 \tag{18b}$$

$$Q_t + \left(\frac{Q^2}{d}\right)_y + \left(\frac{PQ}{d}\right)_x + gdS_y - \frac{1}{3}h^2\left(Q_{yyt} + P_{xyt}\right) = 0 \tag{18c}$$

where d is the total water depth, h is the still-water depth, S is the surface elevation, and P and Q are the depth-integrated velocity components (m^2/s) in the x- and y-direction, respectively. The linear dispersion relation of these equations corresponds to using $B = 0$ in Eq. 15.

As discussed previously, it is a classical procedure to simplify higher order terms by introducing the long-wave equation as a first approximation (see e.g. Mei, 1983). For a mildly sloping sea bed configuration spatial derivatives of the still-water depth can be neglected, and as a first approximation we get:

$$(P_{xxt} + Q_{xyt}) \approx -gh(S_{xxx} + S_{xyy}) \tag{19a}$$

$$(Q_{yyt} + P_{xyt}) \approx -gh(S_{yyy} + S_{yxx}) \tag{19b}$$

Hence, an alternative to Eqs. 18a–c could be obtained by using the approx-

imations from Eqs. 19a–b. In shallow water this would make no difference to the numerical solution, but in deeper water the dispersion characteristics would be very poor, corresponding to using $B=-1/3$ in Eq. 15 (see Fig. 1).

Instead we choose to consider the following quantities:

$$\epsilon_1 \equiv -Bh^2[P_{xxt}+Q_{xyt}+gh(S_{xxx}+S_{xyy})] \tag{20a}$$

$$\epsilon_2 \equiv -Bh^2[Q_{yyt}+P_{xyt}+gh(S_{yyy}+S_{yxx})] \tag{20b}$$

According to Eqs. 19a–b these terms will be insignificant in shallow water and they can be added to the standard Boussinesq equations without affecting the accuracy. By doing so the new equations read:

$$S_t+P_x+Q_y=0 \tag{21a}$$

$$P_t+\left(\frac{P^2}{d}\right)_x+\left(\frac{PQ}{d}\right)_y+gdS_x-(B+\frac{1}{3})h^2(P_{xxt}+Q_{xyt})-Bgh^3(S_{xxx}+S_{xyy})=0 \tag{21b}$$

$$Q_t+\left(\frac{Q^2}{d}\right)_y+\left(\frac{PQ}{d}\right)_x+gdS_y-(B+\frac{1}{3})h^2(Q_{yyt}+P_{xyt})-Bgh^3(S_{yyy}+S_{yxx})=0 \tag{21c}$$

These equations meet the requirements set up at the beginning of this Section with the linear dispersion relation corresponding to Eq. 15 and with group velocities determined by Eq. 17.

In fact, the value of B is not limited to the values discussed previously. Actually, B can be considered as a pure curve fitting parameter in the process of obtaining the best overall agreement with Stokes first-order theory. In Fig. 3, the percentage errors in phase celerity are shown for a number of B values, and it can be seen that it is possible to choose B in such a way as to produce celerities that are improved even compared to Witting's solution of $B=1/15$. For example, choosing the value $B=1/21$ leads to celerity errors less than 3% for the entire range of $0<h/L_0<0.75$ and to group velocity errors (Fig. 2) of less than 6% for the range $0<h/L_0<0.55$.

For completeness, it should be mentioned that additional dispersion can be added to the Eqs. 21a–c by introducing additional terms of the type S_{xxxxx} and P_{xxxxt}. By doing so, it is possible to incorporate Witting's "fourth-order celerity":

$$\frac{c^2}{gh}=\frac{1+\frac{1}{9}k^2h^2+\frac{1}{945}k^4h^4}{1+\frac{4}{9}k^2h^2+\frac{1}{63}k^4h^4} \tag{22}$$

which has a phase celerity error of less than 0.05% at the deep water limit $h/L_0=0.5$. However, the introduction of the additional fifth-order deriva-

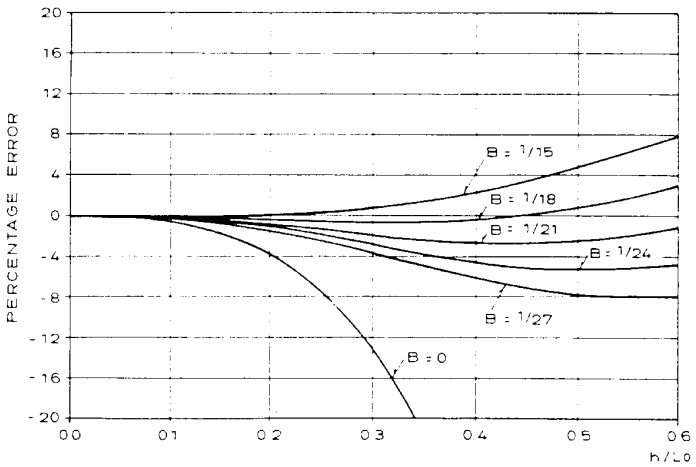

Fig. 3. Percentage errors of the phase celerity, $100(c-c_{STOKES})/c_{STOKES}$, where c is determined from Eq. 15.

tives in the momentum equation currently makes the numerical scheme unattractive from a practical point of view.

4 NUMERICAL SOLUTION

The numerical method used in this paper is based on the socalled SYSTEM 21 scheme which was introduced for tidal modelling by Abbott et al. (1973) and extended to short-wave modelling by Abbott et al. (1978). Since then, this scheme has been under constant development (see McCowan, 1978, 1981; Abbott et al., 1981, 1984).

The differential equations are discretized by using a time-centered implicit scheme with variables defined on a space-staggered rectangular grid. The ADI (Alternative Direction Implicit) algorithm is invoked, and the resulting system of difference equations is reduced to a three-diagonal system, which is solved by the efficient Double Sweep algorithm. The SYSTEM 21 scheme can be illustrated by considering the Boussinesq equations excluding the convective terms. In order to emphasize the time-centering of the scheme, all x- and y-derivatives will be given in their differential form only, since the finite-difference approximation to the spatial derivative is a straight forward mid-centering. In this case, the x-sweep equations read:

$$\left(\frac{S^{n+1/2}-S^{n}}{\frac{1}{2}\Delta t}\right)+\frac{1}{2}\left(P_{x}^{n+1}+P_{x}^{n}\right)+\frac{1}{2}\left(Q_{y}^{n+1/2}+Q_{y}^{n-1/2}\right)=0 \tag{23a}$$

$$\left(\frac{P^{n+1}-P^{n}}{\Delta t}\right)+gd^{*}S_{x}^{n+1/2}-\left(B+\frac{1}{3}\right)\frac{h^{2}}{\Delta t}\left[\left(P_{xx}^{n+1}-P_{xx}^{n}\right)+\right.$$

$$\left(Q_{xy}^{n+1/2}-Q_{xy}^{n-1/2}\right)\Big]-Bgh^3\left(S_{xxx}^{*}+S_{xyy}^{*}\right)=0 \tag{23b}$$

in which $S^{n+1/2}$ and P^{n+1} are the unknown variables. The y-sweep equations read:

$$\left(\frac{S^{n+1}-S^{n+1/2}}{\frac{1}{2}\Delta t}\right)+\frac{1}{2}\left(P_x^{n+1}+P_x^n\right)+\frac{1}{2}\left(Q_y^{n+3/2}+Q_y^{n+1/2}\right)=0 \tag{23c}$$

$$\left(\frac{Q^{n+3/2}-Q^{n+1/2}}{\Delta t}\right)+gd^{**}S_y^{n+1}-(B+\frac{1}{3})\frac{h^2}{\Delta t}\Big[\left(Q_{yy}^{n+3/2}-Q_{yy}^{n+1/2}\right)+$$

$$\left(P_{xy}^{n+1}-P_{xy}^n\right)\Big]-Bgh^3\left(S_{yyy}^{**}+S_{yxx}^{**}\right)=0 \tag{23d}$$

in which S^{n+1} and $Q^{n+1/2}$ are the unknown variables. The * used in Eq. 23b and the ** used in Eq. 23d indicate estimated values at time level $n+\frac{1}{2}$ and $n+1$, respectively. The estimation of the surface elevation on the new unknown time levels is based on an explicit use of the continuity equation. This technique was originally introduced by Abbott et al. (1984) in order to time-center the nonlinear gravity term and the convective terms without using iteration. In order to involve a minimal increase in complexity or computation time relative to the existing model, these estimated surface elevations will be used also to determine the new Boussinesq correction terms S_{xxx}, S_{xyy}, S_{yyy} and S_{yxx}.

This explicit determination of the new terms requires a relatively small time step, especially in deep water where the total Boussinesq effect becomes a balance between relatively large terms. If the time step becomes too large, the result will be a significant damping of the wave energy. The damping increases with increasing values of h/L_0. It turns out that the wave period has to be resolved by approximately 25 time steps in order to avoid the numerical damping. The resolution of the wave length is less restrictive, and normally 8–10 grid points will suffice.

It should be emphasized that alternatives to the explicit estimation of the new terms have been considered. One possibility is to introduce the terms implicitly in the scheme. This can easily be done with the S_{xxx} and S_{yyy} terms, but it will make the momentum operator seven grid points wide and not amenable to simple row elimination to produce a tridiagonal structure. Furthermore, the cross terms S_{xyy} and S_{yxx} cannot be introduced implicitly. Another possibility which has been considered is to apply iteration. This allows for a larger time step to be used, but it turns out that about three iterations are necessary to obtain an accurate solution, which makes the computational effort comparable to or larger than the chosen explicit approach.

At open boundaries, it is essential to take the improved dispersion properties into account. Otherwise, the boundary condition will have the celerity characteristics of the standard Boussinesq equations, which means that waves will not be able to enter the model for h/L_0 larger than 0.48. The calculation of the third spatial derivatives of surface elevation at the first internal flux point requires values of the surface level outside the boundary. These values can be obtained for a flux boundary by applying the surface slope, S_x, together with the depth-integrated velocity, P, as a boundary condition. For a level boundary, the surface curvature, S_{xx}, should be applied together with the surface elevation, S. For waves of constant form on horizontal bottom, S_x and P can be expressed in terms of the surface elevation, the wave frequency and the wave number. Hence, by using Fourier series decomposition techniques, it is possible to determine S_x and P for any linear irregular surface elevation. Similarly, it is possible to determine S_{xx} and S.

5 DISCUSSION OF MODEL RESULTS

Simulations of the propagation of monochromatic waves in a channel with horizontal bottom are shown in Fig. 4a,b. The depth of the channel is 4.2 m and the length is 120 m. At the eastern boundary, waves are absorbed by using a sponge layer. Sinusoidal waves are generated at the western boundary with an incoming wave amplitude of 0.10 m and a wave period of 2.5 s leading to $h/L_0=0.43$. For this value of h/L_0, the standard Boussinesq equations (i.e., $B=0$) lead to a celerity error of -48% and a group velocity error of -90%, while the new equations with $B=1/21$ lead to an error of -3% for the celerity as well as for the group velocity. The use of $B=0$ is illustrated in Fig. 4a, where a western level boundary condition has been applied. Clearly the wave energy is not able to propagate into the model and the wave length is also seen to be too small. The use of $B=1/21$ is illustrated in Fig. 4b, where a western flux boundary has been specified together with the time series of S_x. This is seen to improve the solution dramatically.

In Fig. 5, a bichromatic wave train is simulated. The wave consists of a combination of a 2.5 s wave ($h/L_0=0.43$) and a 3.0 s wave ($h/L_0=0.30$), each having an amplitude of 0.05 m. In the existing model (i.e., $B=0$), the group celerity errors are -90% for the 2.5 s wave and -44% for the 3.0 s wave. Hence, especially the 2.5 s wave is slowed down so much that the resulting time series taken at a position only 12 m down the channel almost looks like a monochromatic wave, at least until the 2.5 s wave eventually reaches the point and re-establishes the bichromatic wave pattern. In the new model (Fig. 5b) with $B=1/21$, the wave train travels down the channel almost undisturbed.

Figure 6 shows a ring test where the waves are generated internally in the center of the model. Absorbing sponge layers are applied along all surround-

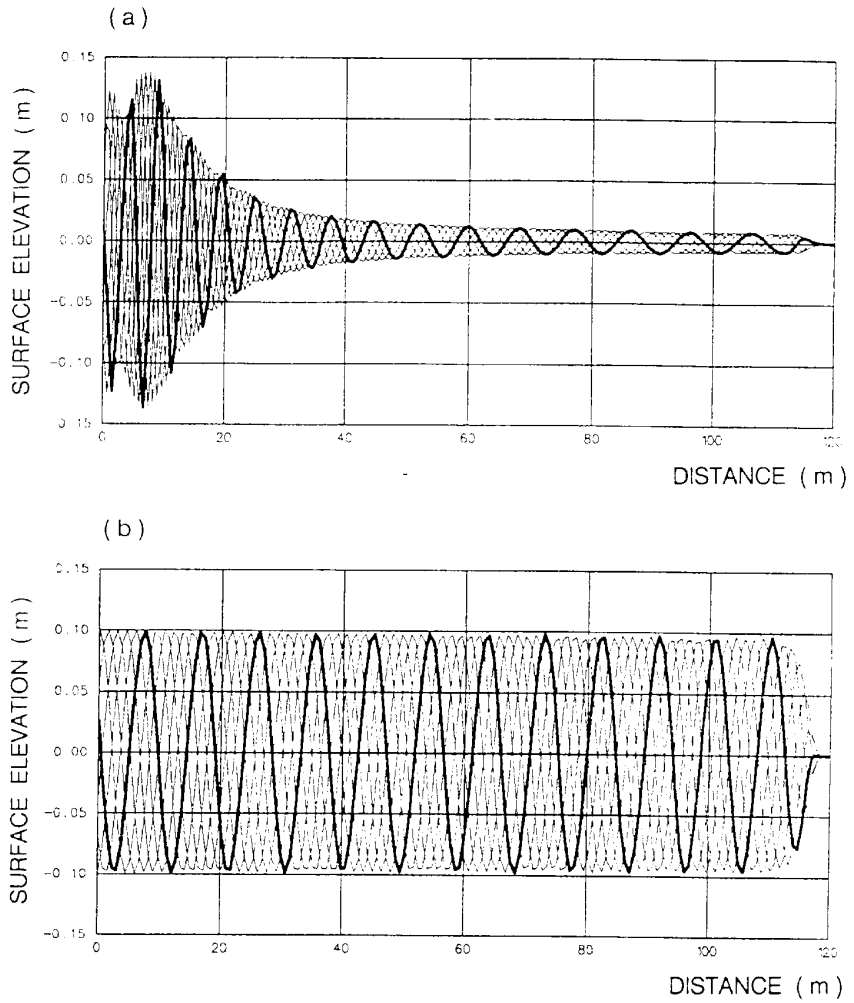

Fig. 4. Monochromatic wave propagation in deep water. Line plots of surface elevation covering one wave period.
(a) Existing model (Abbott et al., 1978).
(b) New model, $B = 1/21$.
Model data: depth = 4.2 m; period = 2.5 s; amplitude = 0.1 m; grid size = 0.75 m; time step = 0.10 s.

ing boundaries. Again, the water depth is 4.2 m and the period is 2.5 s. Figure 6a shows what happens if the cross Boussinesq correction terms, S_{xyy} and S_{yxx} are omitted in the formulation. Now, the wave will propagate with the correct celerity only along the grid lines and not in the diagonal direction. If all Boussinesq correction terms are included, perfectly circular patterns occur (Fig. 6b).

Finally, the new equations have been applied for diffraction in deep water (Fig. 7a–b). The water depth is 40 m and the wave period is 8.0 s, leading to

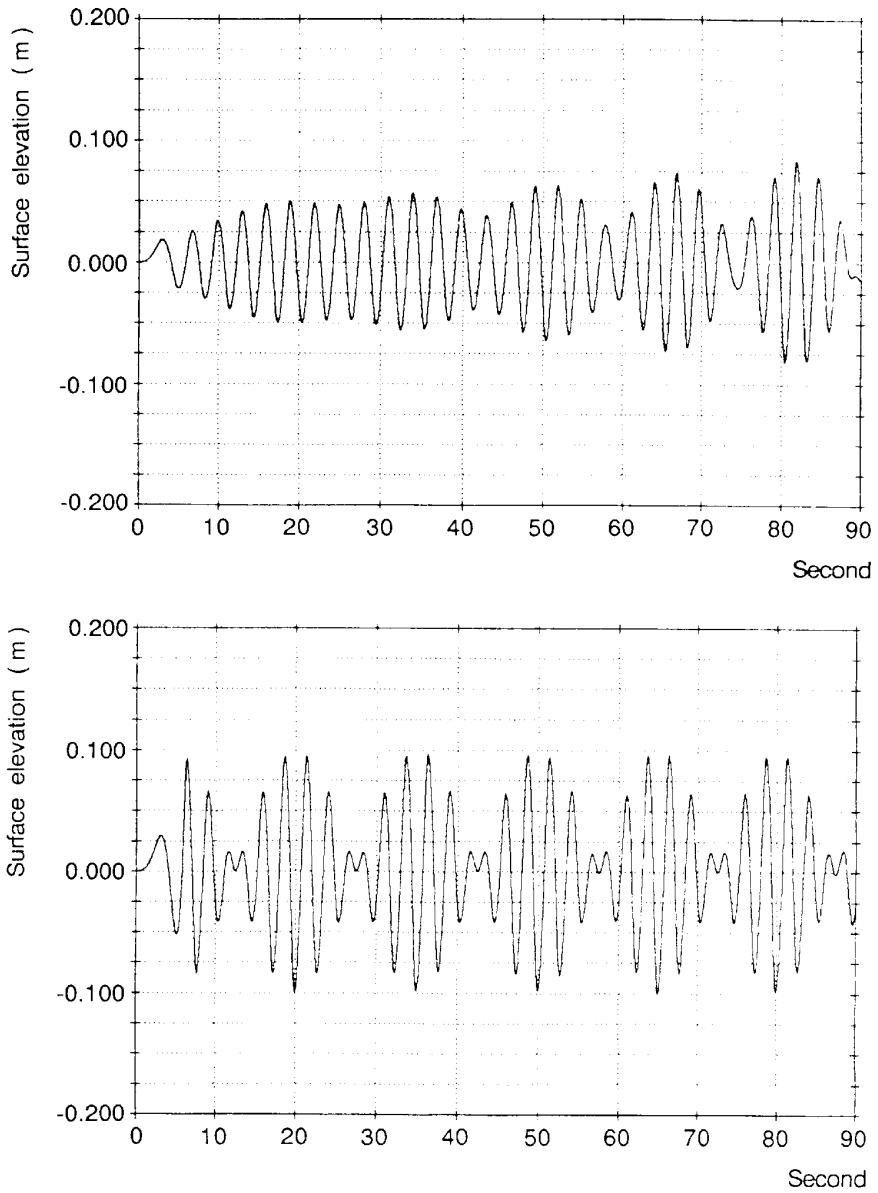

Fig. 5. Bichromatic wave propagation in deep water. Time series of surface elevation 12 m from west boundary.
(a) Existing model (Abbott et al., 1978).
(b) New model, $B=1/21$.
Model data: $a_1=0.05$ m; $a_2=0.05$ m; $T_1=2.50$ s; $T_2=3.00$ s; depth $=4.2$ m; grid size $=0.6$ m; time step $=0.1$ s.

$h/L_0=0.40$. Absorbing sponge layers are applied at the eastern and northern boundaries, while the western boundary (at $x=0$) is fully reflective. Due to the radiation of energy from the point of diffraction, the western boundary

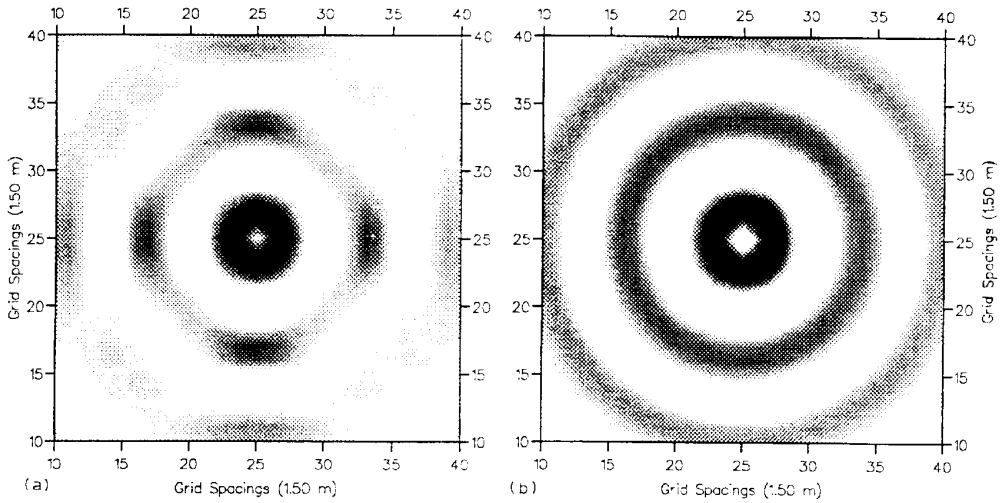

Fig. 6. Circular ring test. Internal wave generation at the center square. Absorbing boundaries.
(a) New model excl. S_{xyy} and S_{yxx} terms.
(b) New model incl. all correction terms.
Model data: depth = 4.2 m; period = 2.5 s; grid size = 1.50 m; time step = 0.125 s; $B = 1/21$.

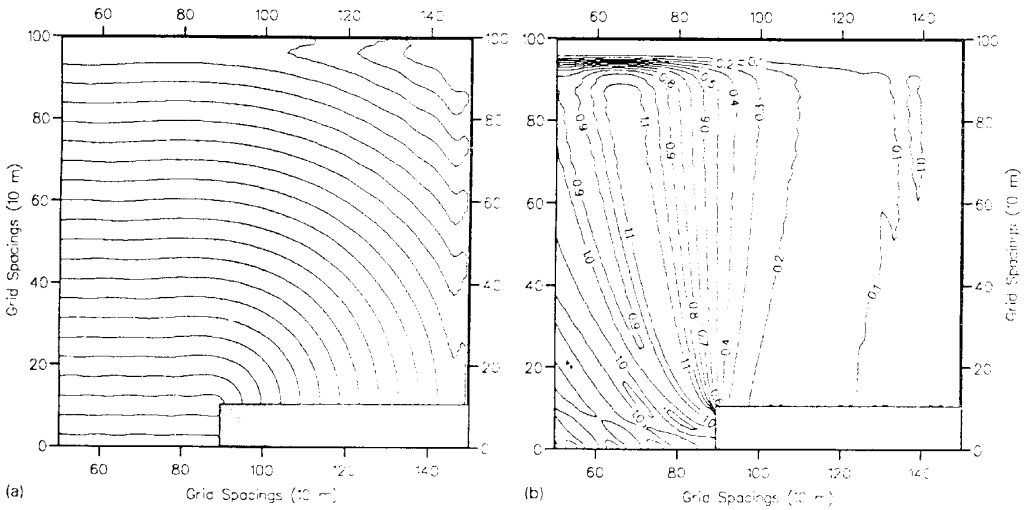

Fig. 7. Diffraction in deep water.
(a) Isolines of zero up- and down-crossings.
(b) Relative wave heights.
Model data: depth = 40 m; period = 8 s; grid size = 10 m; time step = 0.25 s; $B = 1/21$.

has to be placed quite far from the area of interest (eight to nine wave lengths) to avoid reflections in the shadow zone behind the breakwater. The resulting relative wave heights (Fig. 7b) are in perfect agreement with the Shore Protection Manual, which means that the celerity is represented very accurately in the model. This can also be seen from Fig. 7a showing lines of zero up- and down-crossings. The distance between every second isoline corresponds to one wave length, and this is seen to be very close to the expected deep water wave length of 100 m.

6 CONCLUSIONS

In this paper, a new form of the Boussinesq equations has been derived in order to improve the linear dispersion characteristics in deeper water. The improvement is important for studies of wave penetration, refraction and diffraction where the phase celerity and group velocity should be modelled accurately. The new equations make it possible to simulate the propagation of irregular wave trains travelling from deep water (say $h/L_0=0.6$) to shallow water.

It should be emphasized that the new equations are not an attempt to develop a general wave theory valid in deep as well as in shallow water and vertical details like velocity and pressure distributions are not improved relative to the classical equations. Such an improvement would be considerably more complicated and is not within the present scope of work.

Nonlinearities are treated in the classical way by including convective terms and a nonlinear gravity term. The nonlinearities included in this way can be shown to be proportional to the ratio of the wave height to the water depth, H/h. Hence, in deeper water these terms become insignificant and the new equations become effectively linear. In more shallow water, however, the nonlinear properties will be similar to the ones obtained by the standard Boussinesq equations, and waves of up to 75% of their breaking height can be simulated.

This combination of a linear wave model in deep water and a nonlinear wave model in shallow water is justified by the fact that waves which are nonbreaking in shallow water will be only weakly nonlinear in deeper water.

The paper presents a numerical method for solving the new set of equations in two horizontal dimensions without introducing any significant complexity relative to existing Boussinesq models. Model results have been presented for wave propagation and diffraction in relatively deep water, and the obtained accuracy is seen to be most acceptable.

ACKNOWLEDGEMENTS

The authors wish to thank Professor M.B. Abbott for inspiring discussions concerning this work. The work has been supported by the Danish Technical

Research Council through Grant 5.17.7.6.38 and their financial help is gratefully acknowledged.

REFERENCES

Abbott, M.B., Damsgaard, A. and Rodenhuis, G.S., 1973. System 21, Jupiter, A design system for two-dimensional nearly horizontal flows. J. Hydraul. Resour., 11: 1–28.

Abbott, M.B., Petersen, H.M. and Skovgaard, O., 1978. On the numerical modelling of short waves in shallow water. J. Hydraul. Res., 16 (3): 173–111204.

Abbott, M.B., McCowan, A.D. and Warren, I.R., 1981. Numerical modelling of free-surface flows that are two-dimensional in plan. In: Transport Models for Inland and Coastal Water. Symp. Predictive Ability. Academic Press, New York, N.Y.

Abbott, M.B., McCowan, A.D. and Warren, I.R., 1984. Accuracy of short wave numerical models. J. Hydraul. Eng., 110 (10): 1287–1301.

Berenguer, I., Rugbjerg, M., Madsen, P.A. and Kej, A., 1986. Mathematical and physical wave disturbance modelling-complimentary tools. Proc. 20th Int. Conf. Coastal Engineering, 1986.

Chaplin, J.R., 1980. Developments of stream function wave theory. Coastal Eng., 3(3): 179–205.

Larsen, J., Madsen, P.A. and Abbott, M.B., 1984. Numerical modelling of directional seas in deep water. Proc. Symp. Description and Modelling of Directional Seas. Pap. C-2: 11 pp.

Madsen, P.A. and Warren, I.R., 1983. Performance of a numerical short-wave model. Coastal Eng., 8(1): pp. 73–93.

McCowan, A.D., 1978. Numerical simulation of shallow water waves. Proc. 4th Austr. Conf. Coastal and Ocean Eng., Adelaide.

McCowan, A.D., 1981. Developments in numerical short wave modelling. Proc. 5th Aust. Conf. on Coastal and Ocean Eng., Perth.

McCowan, A.D., 1985. Equation systems for modelling dispersive flow in shallow water. Proc. 21st IAHR Congr.

McCowan, A.D., 1987. The range of application of Boussinesq type numerical short wave models. Proc. 22nd IAHR Congr.

Mei, C.C., 1983. The applied dynamics of ocean surface waves. Wiley, New York, N.Y., 740 pp.

Peregrine, D.H., 1967. Long waves on a beach. J. Fluid Mech., 27(4): 815–827.

Peregrine, D.H., 1974. Discussion of: A numerical simulation of the undular hydraulic jump, by M.B. Abbott and G.S. Rodenhuis. J. Hydraul. Res., 12(1): 141–157.

Serre, P.F., 1953. Contribution to the study of permanent and non-permanent flows in channels. La Houille Blanche, pp. 374–388; 830–872.

Svendsen, I.A., 1974. Cnoidal waves over a gently sloping bottom. Tech. Univ. Denmark, Lyngby, ISVA, Ser. Pap. 6.

Whitham, G.B., 1974. Linear and Nonlinear Waves. Wiley, New York.

Witting, J.M., 1984. A unified model for the evolution of nonlinear water waves. J. Comput. Phys., 56: 203–236.

Yu Kuang-Ming, Rugbjerg, M. and Kej, A., 1987. Numerical modelling of harbour disturbances in comparison with physical modelling and field measurements. Proc. 2nd Int. Conf. Coastal and Port Engineering in Developing Countries, Beijing.